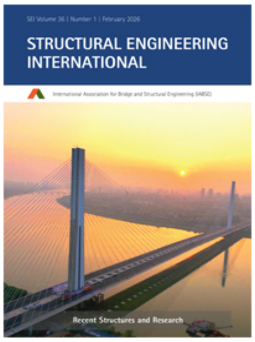

Taylor & Francis
Taylor & Francis Group

Structural Engineering International

ISSN: 1016-8664 (Print) 1683-0350 (Online) Journal homepage: www.tandfonline.com/journals/tsei20

Validity of High-cycle Variable Amplitude Lifetime Estimates of Steel Welded Joints Using Design Models

Marije Deul, Ruben Slange, Henk den Besten & Johan Maljaars Prof. Dr

To cite this article: Marije Deul, Ruben Slange, Henk den Besten & Johan Maljaars Prof. Dr (30 Jan 2026): Validity of High-cycle Variable Amplitude Lifetime Estimates of Steel Welded Joints Using Design Models, Structural Engineering International, DOI: 10.1080/10168664.2025.2610472

To link to this article: https://doi.org/10.1080/10168664.2025.2610472

Published online: 30 Jan 2026.

Validity of High-cycle Variable Amplitude Lifetime Estimates of Steel Welded Joints Using Design Models

Marije Deul, MSc, TNO Department of Naval and Offshore Structures, Delft, the Netherlands; **Ruben Slange**, MSc (PhD Student); **Henk den Besten**, Dr, Marine and Transport Technology, Delft University of Technology, Delft, the Netherlands; **Johan Maljaars**, Prof. Dr, TNO Department Reliable Structures, Delft, the Netherlands; , Built Environment, Eindhoven University of Technology, Eindhoven, the Netherlands. Contact: marije.deul@tno.nl.

DOI: 10.1080/10168664.2025.2610472

Abstract

Increasing demand for the extended lifetime of structures stresses the need for reliable high-cycle fatigue lifetime predictions for variable amplitude-loaded structures. Design standards (including Eurocode 3, AASHTO and British Standard 7608) provide a fatigue design model based on constant amplitude S-N curves and a linear damage accumulation model. There are minor differences in detail categories between standards, but larger differences between the extensions of the S-N curves for variable amplitude loading. It is known that the load spectrum influences this extension due to load interaction and sequence effects. The validity of the predicted fatigue life by available design standards is checked using a compilation of variable amplitude fatigue test data for steel arc-welded joints from the literature with different loading spectra. The results indicate that the standards are generally conservative in the mid- but not in the high-cycle regime, suggesting that resistance non-linearities should be explicitly addressed.

Keywords: fatigue test database; arc-welded joints; design models; variable amplitude load; steel structures; nominal stress.

Introduction

With the increasing demand for the lifetime extension of existing structures, the validity of design curves for the High-Cycle Fatigue (HCF) domain becomes increasingly important. However, the design S-N curves in the HCF domain differ between standards,[1–4] and re-evaluations of the slope and shape of these curves are ongoing in recent years,[5–7] indicating the uncertainty associated with the fatigue evaluation in the HCF domain. Aside from the developments in the S-N curves, the damage accumulation model is also re-evaluated, with some examples of alternatives for the linear damage accumulation model of Palmgren and Miner given by, e.g. Refs. [8–12]. These novel developments have not (yet) made their way to implementation in design standards. This study aims to enhance the understanding of the implications of the differences between standards, based on available Variable Amplitude (VA) fatigue test data.

Fatigue Design Standards

Present-day fatigue designs of welded bridges and similar structures under VA loads are based on the combination of an S-N curve with the linear damage accumulation model of Palmgren and Miner. S-N curves are based on Constant Amplitude (CA) fatigue test data. For VA fatigue, the slope of the curve in the (very) HCF region is typically modified (*Fig. 1*) to incorporate VA effects. This modification involves the extension of the S-N curve below an assumed Constant Amplitude Fatigue Limit (CAFL). The relationship between the applied stress range Δs and the number of cycles to failure N is given by a power law (Basquin equation) as

$$N = A\Delta s^{-m}$$

where $A = A_1$ is a detail-dependent calibration constant for stress cycles above the CAFL, $m = m_1$ is the corresponding slope factor, $m = m_2$ for stress cycles below the CAFL in a VA load spectrum, and the corresponding value $A = A_2$ follows from the other parameters. Slope factor m_1 is typically assumed equal to 3 for steel welded joints subjected to normal stress ranges. An upper- and lower limit assumption for m_2 can be distinguished. The first one is the persistence

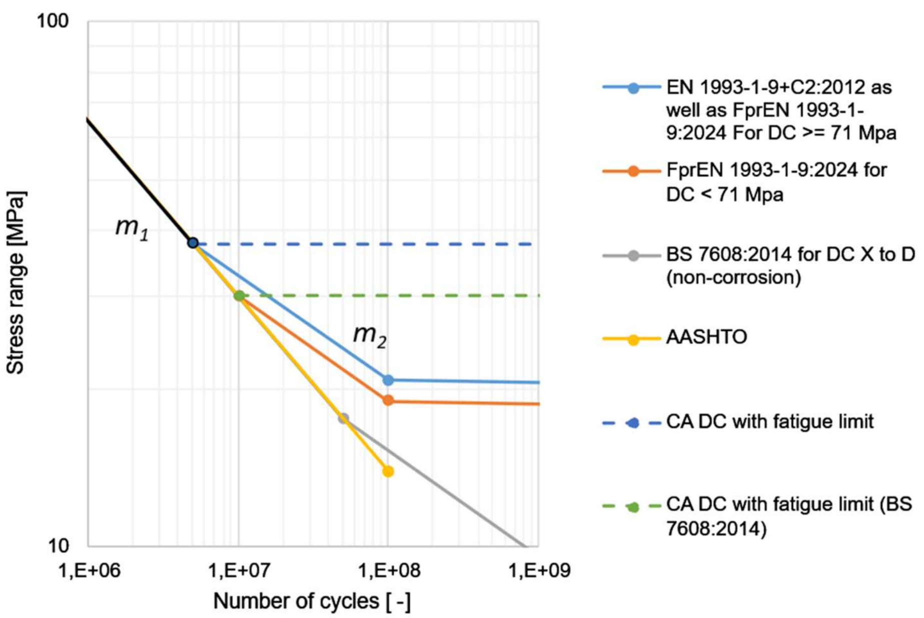

Fig. 1: Design S-N curves for VA loading for an example welded detail, with the CAFL given for reference

of the CAFL (m_2 = Inf), and the second one is a straight continuation of the slope in the CA finite life region (m_2 = m_1). Several standards address the fatigue design of welded joints in steel structures like bridges, such as the current Eurocode EN 1993-1-9:2005,[4] its upcoming successor FprEN 1993-1-9:2024,[3] AASTHO LRFD Bridge Design Specifications[1] and BS 7608:2014.[2] These standards employ comparable values for A_1 and m_1, but larger differences for the other parameters, see *Fig. 1*:

- Standards [1–4] use $m_1 = 3$ for all welded details subjected to normal stress, where [2] uses in general $m_1 = 3$, but $m_1 = 4$ or 3.5 for a limited number of welded details
- Parameter A_1 is defined such that the characteristic S-N curve has an exceedance probability compared to CA test data of 5% for [1,3,4], or 2.5% for [2]. Other small variations in A_1 are attributed to other CA test databases used to infer A_1.
- The slope parameter m_2 = 5 for most details in [2–4] following a proposal by Haibach [13] (m_2 is defined as $m_1 + 2$ in [2]) versus m_2 = 3 [1] if at least one cycle is above the CAFL.
- The slope change location of the curve, further referred to as the knee-point, is taken as the CAFL in [3] and [4]. It is defined at $5 \cdot 10^6$ cycles for all details in [4], whereas [3] defines it at 10^7 cycles or at $5 \cdot 10^6$ cycles for details with low and high fatigue strength, respectively. The knee-point differs from the CAFL in [2], and it is set at $5 \cdot 10^7$ cycles. Note that [1] does not have a knee-point.
- A cut-off value at 10^8 cycles is introduced in [3,4], where fatigue damage induced by stress ranges below the cut-off value is ignored. A cut-off value is not introduced in [2]. Note that [1] does not explicitly account for variable amplitude loading but considers the number of truck passages, by which the continuation of the curve after 10^8 cycles is irrelevant. It is assumed here that the slope $m_2 = 3$ continues over the full domain.
- The critical damage of the linear damage accumulation model is set as $D_{cr} = 1$ [3] and [4]. Contrarily, [2] recommends $D_{cr} = 1$ in general, but adds a note that $D_{cr} = 0.5$ is more realistic for spectra with high tensile loads or if there is uncertainty regarding the service stress spectrum. Note that [1] does not explicitly adopt the linear damage accumulation model. However, it implicitly adopts $D_{cr} = 1$.

None of these standards includes a mean stress correction for welded joints.

Problem Statement and Aim

It is observed by Gurney [14] and others that the calculated critical damage of welded joints depends on the VA load characteristics because of load interaction and load sequence effects. Adopting a fixed critical damage for a broad scope of applications can thus provide a significant error in the predicted fatigue life estimate. However, it would be impractical to formulate a direct spectrum dependency in design standards as the actual spectrum is uncertain in the design stage. A second possibility in the calculation to account for the influence of the VA load characteristics is found in a correction on m_2. Checking the validity of any variation in m_2, damage accumulation model (and critical value), or combination requires VA fatigue test data, but a generally available database is lacking, and the documentation of available data is a known challenge [15].

The aim of this paper is to characterise the differences between the predictions of the fatigue lives of VA fatigue test data from literature using available fatigue design standards in the HCF domain. This is done to conclude the influence of the shape of the design S-N curve in combination with the linear damage accumulation by Palmgren and Miner in available standards for various load histories in the HCF domain.

Database

A database of VA fatigue test results from the literature is drafted to quantitatively compare design models. The requirement adopted here for including test results in the database is that sufficient information is available to enable reproduction, considering:

- Stress spectrum: sufficient information to reconstruct a histogram of the stress and to calculate the mean stress value. Ideally, the formulation enables the reconstruction of an equivalent VA time trace, required for future comparisons with more advanced damage accumulation models.
- Material characterisation: yield stress, steel grade.
- Welding geometry: information to determine the appropriate detail category as per the considered standards.
- Fatigue life: cycles to failure, where failure is defined as a through-thickness crack or complete loss of strength (the difference is neglected in the current study, as it is relatively small for small-scale components loaded in tension).

In addition, the data should be in the scope of the mentioned design standards, implying:

- Specimen base plate thickness equal to or larger than 6 mm.
- Without intended weld imperfections (beyond those allowed for quality level C of ISO 5817:2023 [16]).
- VA load in random sequence representative for bridges and similar structures (excluding CA loads with incident over- or underloads or extreme load peaks compared to the rest of the spectrum).

Finally, only those data are considered with specimens tested in the as-welded state, i.e. without post-weld treatment. *Table 1* provides the database with the references along with their main characteristics, where DC stands for Detail Category, linked to the constant A in Eq. (1).

The present-day fatigue life prediction using the nominal stress method relies on the detailed categories that are defined in the considered standards. The definition of a detail category incorporates the interpretation of a real-world structural detail into standardised categories and thereby reduces uncertainty. For example, the data from Ota [17] and the butt-welded joints from Demofonti et al. [18] are not incorporated in the database, because of insufficient information on the cap size and weld toe angle of the butt-welded joint, which determine the detail category. A second example is that non-destructive testing is required for some detail categories, which increases the confidence in the quality of the weld, whereas the specimen remains unchanged.

Figure 2 presents the distribution of the main properties over the compiled VA fatigue test database: Detail category (DC) for the four considered

Reference	Spectrum	Detail	TT/ TC	DC				No. of tests
				EC [4]	FprEC [3]	BS [2]	AASHTO [1]	
Raftar et al. [17]	Gaussian, constant min	LC cruciform	TT	36	40	W1 (36)	E' (40)	3
Raftar et al. [17]	Gaussian, constant max	LC cruciform	TT	36	40	W1 (36)	E' (40)	4
Grönlund et al. [24]	Gaussian, constant min	NLC longitudinal attachment	TT	71	71	F2 (60)	D (71)	4
Leonetti et al. [21]	Measured bridge replica	NLC cruciform	TT	80	80	E (80)	C (90)	3
Yıldırım et al. [22]	Log-linear	NLC cruciform	TC	80	80	E (80)	C (90)	9
Baptista et al. [23]	Gaussian, constant max	NLC flange tip attachment	TT	40	56	G (50)	E (56)	21
Zhang & Maddox [24]	Concave up, constant max	NLC side attachment	TC	40	56	G (50)	E (56)	4
Zhang & Maddox [24]	Concave up, constant mean	NLC side attachment	TT	40	56	G (50)	E (56)	1
Zhang & Maddox [24]	Concave up, constant min	NLC side attachment	TT	40	56	G (50)	E (56)	1
Zhang & Maddox [24]	Concave up, constant max	NLC longitudinal attachment	TC	56	71	F2 (60)	E (56)	6
Zhang & Maddox [24]	Concave up, constant mean	NLC longitudinal attachment	TT	56	71	F2 (60)	E (56)	2
Zhang & Maddox [24]	Concave up, constant min	NLC longitudinal attachment	TT	56	71	F2 (60)	E (56)	2
Demofonti et al. [18]	Gaussian	NLC cruciform (30mm)	TC	80	80	F (68)	C (90)	26
Demofonti et al. [18]	Gaussian	NLC cruciform (30mm)	TT	80	80	F (68)	C (90)	18
Demofonti et al. [18]	Gaussian	NLC cruciform (10mm)	TC	80	80	E (80)	C (90)	10
Rörup & Petershagen [25]	Log-linear "$R = 0$"[a]	NLC longitudinal attachment	TT	56	71	F2 (60)	E (56)	9
Rörup & Petershagen [25]	Log-linear "$R = -1/3$"[a]	NLC longitudinal attachment	TC	56	71	F2 (60)	E (56)	3
Rörup & Petershagen [25]	Log-linear "$R = -1$"[a]	NLC longitudinal attachment	TC	56	71	F2 (60)	E (56)	7
Rörup & Petershagen [25]	Log-linear "$R = -3$"[a]	NLC longitudinal attachment	TC	56	71	F2 (60)	E (56)	8
Agerskov et al. [26]	BROAD64	NLC longitudinal attachment	TC	56	71	F (68)	E (56)	16
Agerskov et al. [26]	BROAD64	NLC cruciform	TC	80	80	E (80)	C (90)	12
Agerskov et al. [26]	PMMOD64	NLC cruciform	TC	80	80	E (80)	C (90)	10
Klippstein & Schilling [27]	Rayleigh	NLC cruciform	TT	80	80	E (80)	C (90)	10
Fisher et al. [28]	Rayleigh	NLC longitudinal attachment	TT	56	63	F2 (60)	E (56)	35
Fisher et al. [28]	Rayleigh	Cover plate	TT	50	50		E (56)	13

(*Continued*)

Continued.

Reference	Spectrum	Detail	TT/ TC	DC				No. of tests
				EC [4]	FprEC [3]	BS [2]	AASHTO [1]	
						G (50)		
Schilling et al. [29]	Rayleigh	Cover plate	TT	56	56	G (50)	E (56)	9
Schilling et al. [29]	Rayleigh	Welded beam cover plate	TT	56	56	G (50)	E (56)	6
Yamada & Albrecht [30]	Bridge load replication	Cover plate tapered ends	TT	56	56	G (50)	E (56)	54
Yamada & Albrecht [30]	Bridge load replication	Welded beam tapered flange butt weld	TT	71	90	D (90)	B' (100)	66
							Total	**372**

[a]For the dataset of Rörup and Petershagen [25], there are four different mean stress levels, indicated by the values R between 0 and −3 as used in [25]. However, these values only refer to the largest stress range in the load sequence, and they are therefore put between quotation marks.

Table 1: Database specification, indicating the spectrum, detail type, tension-tension (TT) or tension-compression (TC) load, detail categories according to the standards and the number of tests

standards, failure location, publication year, yield strength, base plate thickness, runout/failure and global mean stress of the time trace. The figure shows that the data are not uniformly distributed over the different categories. For example, the global mean stress is skewed towards zero, indicating that partly compressive cycles are not uncommon.

Results: Fatigue Life Prediction

The fatigue life of the specimens in the database is predicted using the design

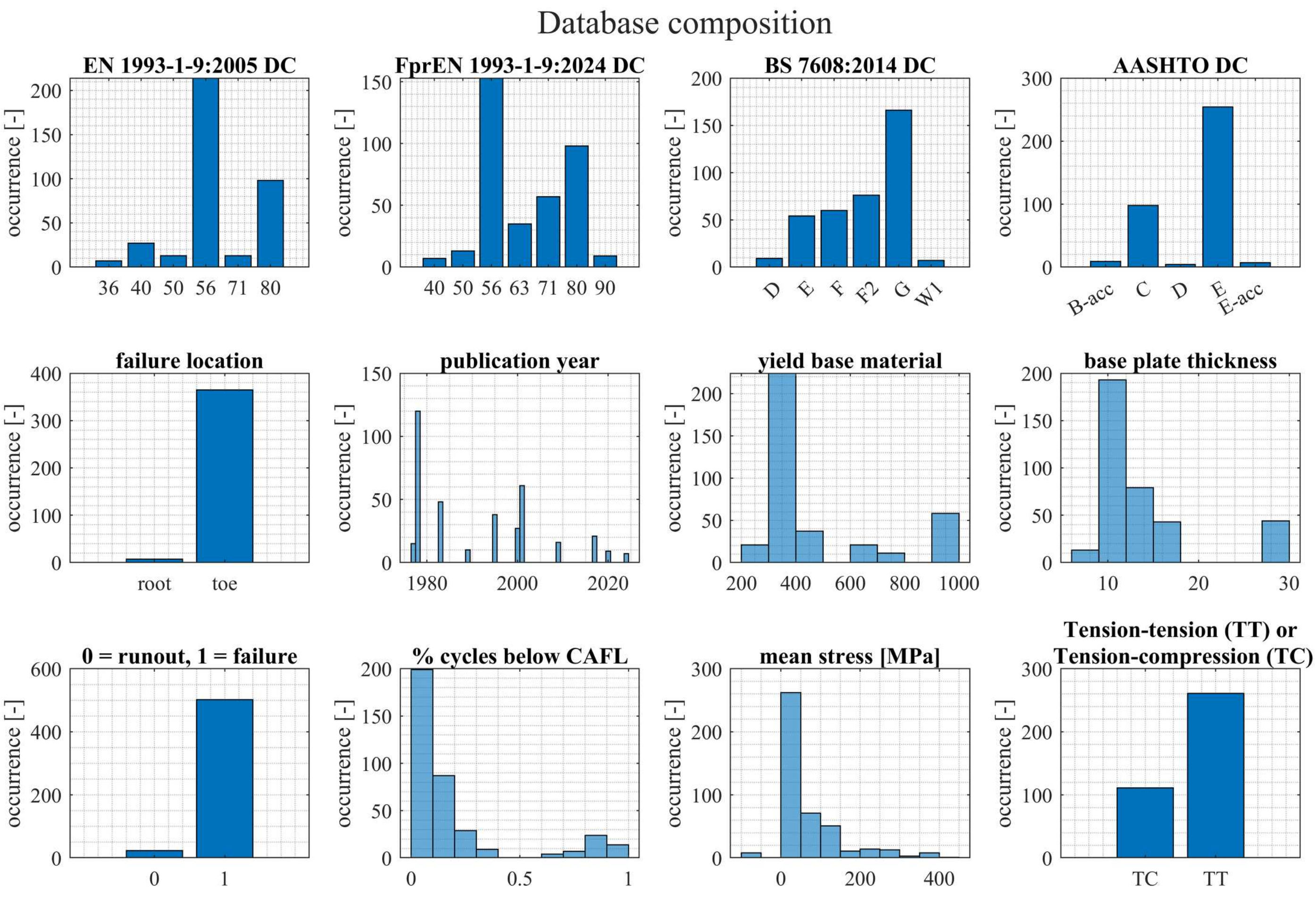

Fig. 2: Database composition visualisation

models in the previously mentioned standards.[1–4] The S-N curves in standards are based on tension-tension fatigue test data. For this reason, in addition to the analysis of the full database, a subset is evaluated with tension-tension VA data only. The resulting predicted fatigue lives using the four design models are compared to the experimentally determined fatigue lives using characteristic and mean (if available) S-N curves in *Fig. 3* per dataset. BS 7608:2014 [2] provides both the design and the mean fatigue resistance, but this information is lacking in the other standards. The mean curve for the FprEN 1993-1-9:2024 [3] is obtained from the collected data from which the DCs are derived in [31]. The data is shown again in *Fig. 4* with a colour bar indicating the fraction of cycles below the CAFL. Note that the applied CAFL is at $5 \cdot 10^6$ cycles, which is not in line with all standards, see Section 1. However, the exact value of the CAFL does not influence the visual presentation of the results. As a measure of the quality of the fit (i.e. how well the respective standards predict the experimental fatigue life), the standard deviation of the mean life predictions is calculated and presented in the plot headers.

It can be observed from *Figs. 3 and 4* that the fatigue life of the dataset by Fisher [28] is, on average, overpredicted by all standards and that this dataset has significantly more cycles below the CAFL than other datasets. Upon excluding the dataset by Fisher [28], the standard deviations of the logarithmic mean life predictions σ change from 0.84 to 0.75 and are fixed at 0.80 for FprEN 1993-1-9:2024 [32] and BS 7608:2014 [2], respectively. The mean critical damage μ changes from 1.08 to 1.11 and from 1.10 to 1.12 for both standards. This indicates that the prediction is, on average, more conservative and less scattered when excluding the data from Fisher.

The change of the location of the slope change from the current Eurocode EN 1993-1-9:2005 [4] to a differentiation for detail categories above and

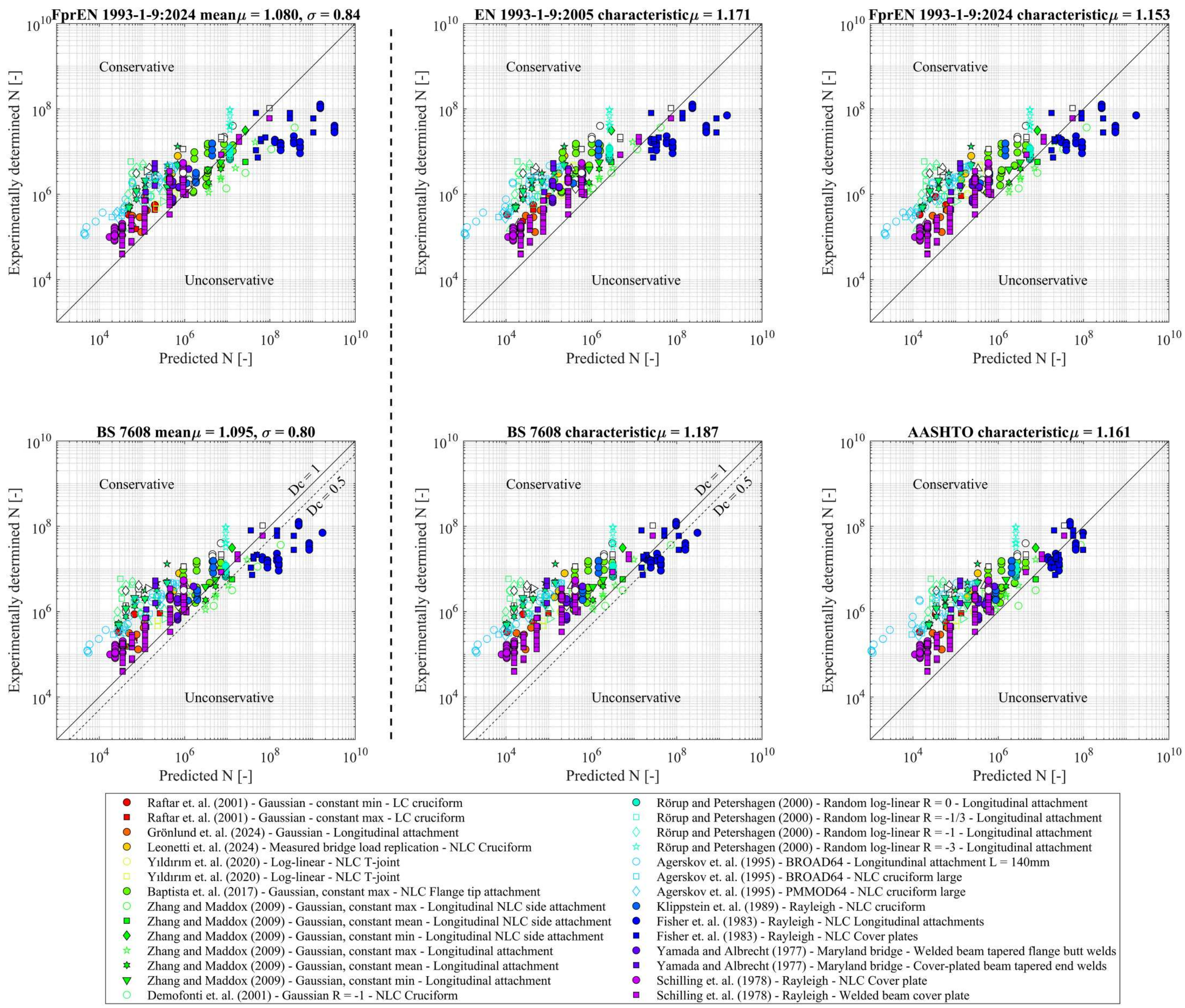

Fig. 3: Comparison between the experimentally determined and predicted fatigue life considering the mean and characteristic S-N curves of four different standards of all data in the dataset. White markers indicate a runout. Open markers indicate TC data, where filled markers indicate TT data

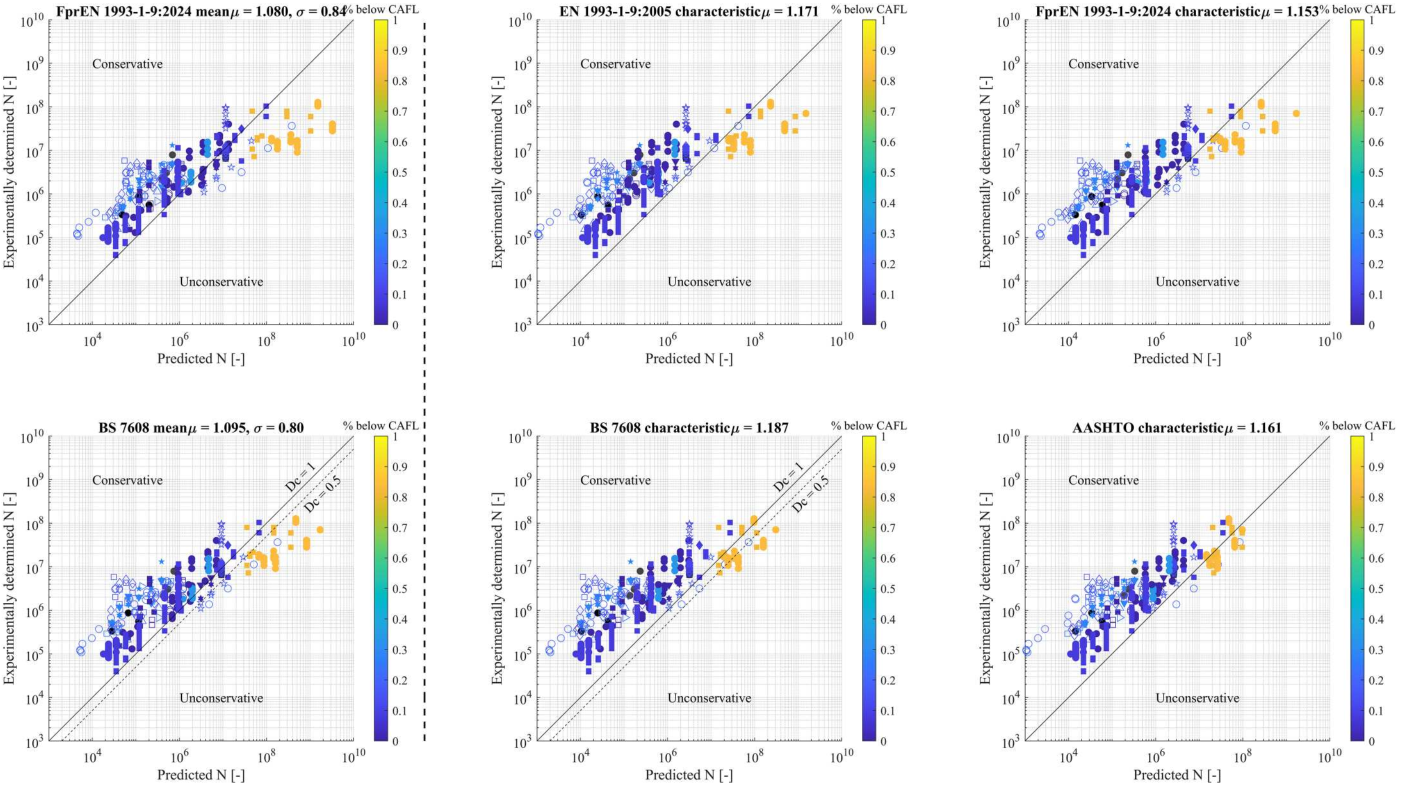

Fig. 4: Comparison between the experimentally determined and predicted fatigue life considering the mean and characteristic S-N curves of four different standards of all datapoints in the dataset. Open markers indicate TC data, where filled markers indicate TT data

below DC 71 in the upcoming version FprEN 1993-1-9:2024 [3], in combination with changes to the DCs, slightly improves the prediction. However, both Eurocode versions give a worse prediction than BS 7608:2014 [2] and AASHTO [1], both in terms of percentage of overpredicted datapoints and their average deviation.

On average, the predicted fatigue lives of TC VA data are more conservative than the TT data. The generally applied assumption for welded joints is that the tensile residual stress at locations of crack initiation is so high that the mean stress of the cycles is irrelevant. However, under cyclic loading, relaxation of these residual stresses leads to longer lives.[33] In VA loading, this effect may be more prominent than in CA loading due to load sequence effects, where large stress cycles can cause residual stress relaxation, affecting the damage induced by subsequent smaller cycles.[34] Such a mean stress correction is not posed in the considered standards for welded joints, causing the more conservative results for the TC data.

Table 2 provides indicators for the performance of the standards. The first columns give the mean critical damage, defined as the mean of the ratios between the predicted number of cycles using (when available) the mean S-N curve and the experimental number of cycles. The centre columns present the fraction of data for which the characteristic S-N curves result in an overpredicted fatigue life, along with a colour to indicate whether the value is higher or lower than the exceedance probability associated with the characteristic value of each

Standard	Mean critical damage based on the mean S-N curve (when available)			Exceedance probability associated with the characteristic curve	Fraction overpredicted			Average deviation of overpredicted values $1-\frac{N_{\mathrm{exp}}}{N_{pred}}$		
	All data	Excl. TC	Excl. Fisher		All data	Excl. TC	Excl. Fisher	All data	Excl. TC	Excl. Fisher
EN 1993-1-9:2005				5%	13%	18%	1%	6.5%	6.8%	0.7%
FprEN 1993-1-9:2024	1.08	10.5	1.11	5%	16%	18%	3%	6.1%	6.7%	3.7%
BS 7608:2014 ($D_c = 1$)	1.10	1.07	1.12	2.5%	9%	11%	1%	5.0%	5.2%	3.5%
AASHTO				5%	9%	12%	2%	3.2%	3.0%	4.4%

Table 2: Mean critical damage, fraction of datapoints with a predicted life using characteristic values exceeding the experimental life and average deviation of the overpredicted values. The coloured boxes indicate the best (green) to worst (red) performing datasets and standards

standard. As a measure of the extent of overprediction, the average deviation, expressed by the average value of $1 - \frac{N_{exp}}{N_{pred}}$, of the overpredicted values is presented in the final columns. *Table 2* indicates the large influence of excluding the dataset from Fisher [28], where the exclusion of this dataset results in a percentage of overpredicted values that stays within the bounds of the standards. It is to be mentioned that safety factors are not accounted for, which does not necessarily indicate unsafe designs, as further elaborated below. The AASTHO [1] results for all data have a relatively small fraction of overpredicted values, and the average deviation is the smallest if Fisher's data is excluded.

Discussion

(Almost) the entire fatigue damage of the brightest datapoints in *Fig. 4* is created in the part of the S-N curve above the CAFL, i.e. the part with slope parameter m_1. The characteristic predicted lives of these data are, on average, shorter than the experimental lives for all four design models. Contrarily, for a high fraction of cycles below the CAFL, the predicted lives are longer than the experimental values. Guidelines and standards such as British Standard [2] and IIW [35] recommend the use of a critical damage lower than 1 to reduce the fraction of too optimistic predictions. However, the above observation implies that such a simple adjustment is not advisable, as this would make the underpredicted datapoints even more conservative, resulting in overconservative designs in the mid-cycle domain. It seems more appropriate to adjust the slope parameter m_2, because this affects only the cycles below the CAFL.

A lower location of the (knee-point of the) second slope of the S-N curve (as is done in the variations of BS 7608 and AASHTO) is shown to decrease the fraction of overpredicted data, indicating a fatigue limit degradation under VA loading conditions. The AASTHO design model has the smallest difference between the overpredicted fraction and the target fraction, and the average deviation of the overpredicted data is the lowest, indicating that if there is an overprediction, it is not as severe as in the other design models. This further supports the reconsideration of the slope parameter m_2.

Fisher's [28] data stand out for multiple reasons. Aside from the small number of cycles with a range exceeding the CAFL, as mentioned above, the two details (longitudinal attachment and cover plate) have a relatively low DC, frequently encountered in existing bridges but usually not applied in new designs. Further, this dataset is relatively old compared to the other data, with the welding process applied at that time potentially influencing weld imperfections and residual stress. Finally, the specimens are from steel grade A514, with a nominal yield stress of approximately 700 MPa, whereas most other data are from steels of lower grade. Further experimental studies should be conducted to determine which of these deviations is (or are) responsible for the differences in predicted fatigue lives compared to the other datasets. Such a study would give insight into the applications for which the current design models can be used straightforwardly, and for which adaptations are required. Note that Fisher's [28] data are considered in the evaluation of the partial (safety) factors of FprEN 1993-1-9:2024 [3], as outlined in Ref. [36]. The required partial safety factors according to that study are slightly higher than those adopted in the upcoming Eurocodes, but the deviation is mainly attributed to the load model, which requires calibration per country. Hence, the overprediction of the fatigue lives in this paper (excluding a partial safety factor) of Fisher's [28] data does not immediately pose a safety issue.

The database size is limited to-date, with many of the datasets having a load spectrum where the vast majority of the fatigue damage is created above the CAFL, unsuited to evaluate the slope parameter m_2. Further, *Fig. 2* shows that the database composition is not evenly distributed over different properties. The considered weld root failure datapoints [19] are within the scatter band of the weld toe failures, although the weld root failure database is too small to draw generic conclusions. The results should, therefore, be used as indicative only. Quantitative conclusions on the influence require a more extensive database. Finally, most VA loads are synthetic, e.g. follow standard distributions (Gaussian, Rayleigh, log-linear, etc) with often block-loaded sequences and a single frequency component. It is recommended to conduct tests with more random load histories that are representative of bridges and other types of structures covered by the standards.

Conclusions

The following conclusions are drawn:

- All four design models (without additional safety factors) have more data with overpredicted lives using the characteristic S-N curves than the exceedance probability associated with the characteristic value of the respective standards. Upon excluding the data by Fisher [28], which has only between 0.2 and 12% of the cycles above the CAFL, the overprediction probability is within the target. This indicates that small stress ranges do matter to the damage.
- The current design models are all conservative for load spectra containing a majority of stress cycles above the CAFL. However, BS 7608 [2], and in particular (Fpr)EN 1993-1-9 [3,4], which has a cut-off value, give unconservative predictions for load spectra containing only a few cycles above the CAFL, which are highly relevant to practice. AASHTO [1], although not explicitly considering VA loads, uses single-slope S-N curves and generally provides a better fit. This indicates that the application of a correction on the critical damage is not advisable, as this imposes the same correction on all data points. A selection of the slope parameter m_2 closer to m_1 that of AASHTO [1] seems more suitable.
- Contrary to EN 1993-1-9:2005 [4], the new standard FprEN 1993-1-9:2024 [3] specifies differentiation of the number of cycles at the CAFL for details with a high and a low DC. This is in addition to a change in several of the detail categories. This differentiation provides a small improvement in the predictions.

Acknowledgements

The authors acknowledge the financial support from the Dutch Ministry of Infrastructure and Water Management.

Author Contributions

Marije Deul: Conceptualisation, Formal Analysis, Investigation, Data Curation, Writing—Original Draft, Visualisation. Ruben Slange: Investigation, Writing—Review & Editing. Henk den Besten: Writing—Review & Editing. Johan Maljaars: Conceptualisation, Writing—Review & Editing.

Disclosure Statement

No potential conflict of interest was reported by the author(s).

Data Availability Statement

The variable amplitude fatigue test database [37] is published under the following doi:10.5281/zenodo.17183982.

ORCID

Marije Deul http://orcid.org/0009-0008-4141-9963
Ruben Slange http://orcid.org/0009-0004-3030-9321
Henk den Besten http://orcid.org/0000-0002-8726-218X
Johan Maljaars http://orcid.org/0000-0001-5831-2478

References

[1] AASHTO. AASHTO LRFD bridge design specifications. Washington (DC): AASHTO, 2007.

[2] British Standards. BS 7608:2014 Guide to fatigue design and assessment of steel products, BSI, 2014.

[3] CEN. FprEN 1993-1-9:2023 (E) Eurocode 3: design of Steel Structures – Part 1-9: fatigue. Brussels: CEN, 2023.

[4] CEN. EN 1993-1-9 Eurocode 3: design of Steel Structures – Part 1-9: fatigue. Brussels: CEN, 2005.

[5] Lotsberg I. Derivation of design S-N curves for butt welds in support structures for wind turbines. Mar Struct. 2025; 102: 103795.

[6] Mehmanparast A, Chahardehi A, Brennan F, Manzocchi M. Re-evaluation of fatigue design curves for offshore wind monopile foundations using thick as-welded test specimens. Eng Fail Anal. 2024; 158: 107971.

[7] Qin Y, den Besten H, Palkar S, Kaminski M. Mid-and high-cycle fatigue of welded joints in steel marine structures: effective notch stress and total stress concept evaluations. Int J Fatigue. 2021; 142: 105822.

[8] Hirt MA, Kunz PM. Fatigue safety of existing steel bridges. Int J Fatigue. 1998; 65(11): 399–406.

[9] Leonetti D, Maljaars J, Snijder H. Probabilistic fatigue resistance model for steel welded details under variable amplitude loading – inference and uncertainty estimation. Int J Fatigue. 2020; 135: 105515.

[10] Rege K, Pavlou D. A one-parameter nonlinear fatigue damage accumulation model. Int J Fatigue. 2017; 98: 234–246.

[11] Ray Asok, and Ravindra Patankar Fatigue crack growth under variable-amplitude loading: Part I-Model formulation in state-space setting. *App Mathe Mod.* 2001; 25(11): 979–994.

[12] Newman JC, Brot A, Matias C. Matias Crack-growth calculations in 7075-T7351 aluminum alloy under various load spectra using an improved crack-closure model. *Eng Fract Mech.* 2004; 71: 2347–2363.

[13] Haibach E. Modifizierte lineare Schadensakkumulations-Hypothese zur Berücksichtigung des Dauerfestigkeitsabfalls mit fortschreitender Schädigung, LBF-Technische Mitteilung TM 50/70. Fraunhofer Institut für Betriebsfestigkeit – LBF, Darmstadt, 1970.

[14] Gurney T. The influence of narrow band, wide band and service loading. In Cumulative damage of welded joints, Cambridge, England: Woodhead, 2006; 147–192.

[15] Hectors K, Vanspeybrouck D, Plets D, Bouckaert Q, De Waele W. Open-access experiment dataset for fatigue damage accumulation and life prediction models. Metals (Basel). 2023; 13: 621.

[16] ISO. ISO 5817:2023 welding – fusion-welded joints in steel, nickel, titanium and their alloys (beam welding excluded) – Quality levels for imperfections, ISO, 2023.

[17] Ota A, Maeda Y, Suzuki N. Fatigue strength of transverse butt welded joints under random loading. Application of miner's rule in smax=sy tests. Weld Int. 1997; 11(12): 958–965.

[18] Demofonti G, Riscifuli S, Sonsino CM, Kaufmann H, Sedlacek G, Müller C, Hanus F, Wegmann HG. High-strength Steels in Welded State for Lightweight Constructions Under High and Variable Stress Peaks. Brussels: European Commission, 2001.

[19] Raftar H, Ahola A, Lipiäinen K, Björk T. Fatigue behavior of load-carrying cruciform fillet weld joints under variable amplitude load. J Constr Steel Res. 2024; 215: 108559.

[20] Grönlund K, Ahola A, Riski J, Pesonen T, Lipiäinen K, Björk T. Overload and variable amplitude load effects on the fatigue strength of welded joints. Weld World. 2024; 68: 411–425.

[21] Leonetti D, Kinoshita K, Takai Y, Nussbaumer A. Fatigue behavior of transverse attachments under contant and variable amplitude loadig from a Swiss motorway bridge. Int J Fatigue. 2024; 178: 108003.

[22] Yıldırım HC, Remes H, Nussbaumer A. Fatigue properties of as-welded and post-weld-treated high-strength steel joints: the influence of constant and variable amplitude loads. Int J Fatigue. 2020; 138: 105687.

[23] Baptista C, Reis A, Nussbaumer A. Probabilistic S-N curves for constant and variable amplitude. Int J Fatigue. 2017; 101: 312–327.

[24] Zhang Y-H, Maddox S. Investigation of fatigue damage to welded joints under variable amplitude loading spectra. Int J Fatigue. 2009; 31: 138–152.

[25] Rörup J, Petershagen H. The effect of compression mean stresses on the fatigue strength (IIW Document No. XIII-1785-99). IIW German Delegation, 2000.

[26] Agerskov H, Petersen RI, Lopez Martinez L, Askegaard V. Fatigue life of high-strength steel plate elements under stochastic loading. Lyngby: Technical University of Denmark; 1995.

[27] Klippstein K, Schilling C. Pilot study on the constant and variable amplitude behavior of transverse stiffener welds. J Constr Steel Res. 1989; 12: 229–252.

[28] Fisher J, Mertz D, Zhong A. Steel Bridge Members Under Variable Amplitude Long Life Fatigue Loading (NCHRP Report 267). Washington (DC): Transportation Reserach Board, National Research Council, 1983.

[29] Schilling C, Klippstein K, Barsoum JM, Blake G. Fatigue of Welded Steel Bridge Members Under Variable-Amplitude Loadings (NCHRP Report 188). Washington (DC): Transportation Research Board, National Research Council, 1978.

[30] Yamada K, Albrecht P. Fatigue behavior of two flange details. J Struct Div. 1977; 103(4): 781–791.

[31] Feldmann M, Ummenhofer T, Kuhlmann U. Forschungsbericht - Neubewertung und Erweiterung des Kerbfallkatalogs nach Eurocode 3 für eine zukunftsfähige Auslegung hochbeanspruchter Stahlkonstruktionen, DASt, Stuttgart, 2019.

[32] CEN. prEN 1993-1-9:2023 (E) Eurocode 3: design of Steel Structures – Part 1-9: fatigue. Brussels: CEN, 2023.

[33] Hensel J. Einfluss von Schweis seigenspannungen auf den Schwingfestigkeitsnachweis von Schweissverbindungen im Nennspannungskon zept. [dissertation]. Shaker Verlag, 2017.

[34] Anderson TL. Fracture mechanics. Boca Raton: CRC Press, 2017.

[35] Hobbacher A. Recommendations for fatigue design of welded joints and components, IIW, Springer, 2018.

[36] Maljaars J, Leonetti D, Hashemi B, Snijder BH. Systematic derivation of safety factors for the fatigue design of steel bridges. Struct Saf. 2022; 97: 102229.

[37] Deul ML, Slange RLG. Supplementary material: MATLAB database variable amplitude fatigue tests in reference. Validity of high cycle variable amplitude lifetime estimates of steel welded joints using design models, 2025. doi:10.5281/zenodo.17183982.